

## Measurement of $\Lambda^0$ Polarization in Inclusive $\Lambda^0$ Production at 28.5 GeV/c

F. Lomanno, D. Jensen, M. N. Kreisler, R. Poster,<sup>(a)</sup>

M. S. Z. Rabin, M. Way,<sup>(b)</sup> and J. Wise<sup>(c)</sup>

*Department of Physics and Astronomy, University of Massachusetts, Amherst, Massachusetts 01003*

and

J. Humphrey

*Brookhaven National Laboratory, Upton, Long Island, New York 11973*

(Received 16 October 1979)

$\Lambda^0$  polarization in inclusive production by protons on iridium has been measured at 28.5 GeV/c over the region  $0.55 \text{ GeV}/c \leq P_{\perp} \leq 1.6 \text{ GeV}/c$ . The polarization rises from  $(-12.6 \pm 5.5)\%$  at 0.55 GeV/c to  $(-33.4 \pm 4.6)\%$  at 1.6 GeV/c. Significant differences from previous measurements at other energies with different targets are observed, particularly at low  $P_{\perp}$ .

Recent studies<sup>1-3</sup> of inclusive  $\Lambda^0$  production have shown that the  $\Lambda^0$ 's have significant polarization. Although the source of this polarization is not understood, there are at present three models which attempt to explain the phenomenon: the gluon bremsstrahlung model of Heller,<sup>3,4</sup> the model of Andersson *et al.*<sup>5</sup> which requires  $q\bar{q}$  pairs to be produced in the color field, and a model involving the interference between nearby  $\Lambda^0$  excited states.<sup>6</sup> In order to provide more information on the energy, target material, and transverse-momentum dependence, to test the predictions of these various models, as well as to observe the effect independently, we have conducted a measurement of  $\Lambda^0$  polarization in inclusive  $\Lambda^0$  production using 28.5-GeV/c protons. The  $\Lambda^0$  polarization was determined by a measurement of the decay  $\Lambda^0 \rightarrow p + \pi^-$ .

The experiment was performed at Brookhaven National Laboratory with the apparatus shown in Fig. 1. Protons from the external beam of the alternating-gradient synchrotron (28.5 GeV/c) interact in an iridium target (2.5 mm square  $\times$  76 mm long). A neutral beam was defined at  $4^\circ$  with respect to the proton beam by a 500- $\mu$ sr solid-angle collimator, positioned in the field of a sweeping magnet (D5) which removed charged particles. A 10-radiation-length Pb filter removed

photons, leaving a neutral beam consisting mainly of  $\Lambda$  particles, kaons, and neutrons. A veto counter (HV) ensured that a neutral particle entered the vacuum box.

The spectrometer consisted of two analyzing magnets in order to measure the laboratory momenta of the pion and proton with comparable precision. Track trajectories were measured using 28 electronic-readout spark-chamber planes. The pion was momentum analyzed in D6, a dipole magnet with a field integral of 3.25 kG m, and the proton was momentum analyzed in D7, a dipole magnet with field integral of 27.0 kG m.

Information from five hodoscope banks (HF, HMX, HMY, HRX, HRY), two "proton" counters (HP1, HP2) and the veto counter (HV) was used in defining our trigger. HMX and HMY had a hole at the proton aperture. The basic trigger (2T) demanding two tracks (one long and one short) in the spectrometer was defined as

$$2T = \overline{HV} \cdot HF \cdot (HMX + HMY)$$

$$\cdot (HRX + HRY) \cdot HP1 \cdot HP2.$$

There were four gas-filled atmospheric-pressure threshold Cherenkov counters (CE1, CE2, C $\pi$ 1, C $\pi$ 2) which were used for particle identification. Par-

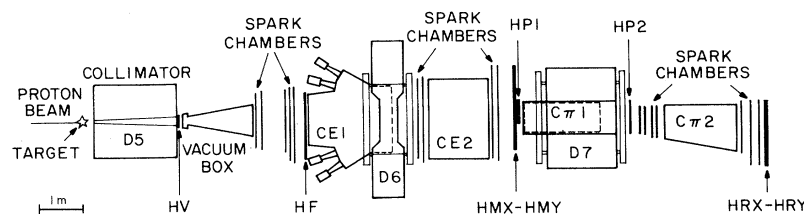


FIG. 1. Layout of the experimental apparatus.

ticle identification was not used in the 2T trigger requirement from which the  $\Lambda^0 \rightarrow p\pi^-$  sample was extracted. This eliminated one source of possible bias in the acceptance. The data presented here are based on a sample of  $3.08 \times 10^6$  triggers.

The trigger requirement was sufficiently unconstrained to measure scintillation-counter and spark-chamber efficiencies internally from the data. Special runs were taken to measure the efficiencies of the proton counters. A separate trigger,  $2T \cdot (C\pi 1 + C\pi 2)$ , was used to accumulate a sample of the decay  $K_s^0 \rightarrow \pi^+\pi^-$ , which was used to search for possible biases in the spectrometer.

All events were processed by a computer track-finding program. All events were required to have a decay vertex inside the vacuum decay region, to have both track trajectories satisfy geometrical cuts, to have the distance of closest approach of the two tracks at the vertex be consistent with the chamber resolutions, and to have the vector momentum of the two tracks point back to the production target.

The invariant-mass distribution, based on the assumption that the long positive track is a proton and that the short negative track is a pion, is shown in Fig. 2(b). The  $\Lambda^0$  peak with a mass resolution of  $\sigma = 2.3 \text{ MeV}/c^2$  and with negligible background is evident. There are 430 000  $\Lambda^0$ 's within  $\pm 3\sigma$  of  $M_{\Lambda^0} = 1115.5 \text{ MeV}/c^2$ . The momentum spectrum of these events is shown in Fig. 2(a).

The geometrical acceptance for each event was calculated with a Monte Carlo program, which included such effects as multiple Coulomb scattering,  $\pi \rightarrow \mu\nu$  decays in flight, and the measured counter/spark chamber efficiencies. Monte Carlo-generated events were processed through the same track-finding and analysis programs as the data. Comparisons were made between Monte

Carlo-generated events and the data in distributions such as track momenta, invariant mass, illuminations at detector planes, location of the decay vertex, and target pointback. All comparisons had very good  $\chi^2$  agreement.

The coordinate system chosen for the polarization measurement was defined as follows: The  $\hat{z}$  axis is normal to the  $\Lambda^0$  production plane ( $\hat{z} = \hat{P}_b \times \hat{P}_\Lambda$ , where  $\hat{P}_\Lambda$  and  $\hat{P}_b$  are unit vectors along the  $\Lambda^0$  and incident proton beam, respectively.); the  $y$  axis is along  $\hat{P}_\Lambda$ ; and  $\hat{x}$  is chosen to form a right-handed coordinate system. The angle  $\theta$  is defined in the  $\Lambda^0$  center-of-mass system by the angle between the decay proton and the  $\hat{z}$  axis.  $\varphi$  is the polar angle defined with respect to the  $\hat{x}$  axis. All of the data events were binned according to the  $\Lambda^0$  transverse momentum,  $\cos\theta$ , and  $\varphi$ .

The  $\Lambda^0$  decay is self-analyzing for polarization in the decay mode  $\Lambda^0 \rightarrow p + \pi^-$ . The decay-proton distribution in the  $\Lambda^0$  center of mass relative to the  $\Lambda^0$  spin direction is given by<sup>7</sup>

$$dW/d\Omega = (1 + \alpha\mathcal{P}\cos\theta)/4\pi, \quad (1)$$

where  $\alpha = 0.642$  (Ref. 8) and  $\mathcal{P}$  is the polarization of the  $\Lambda^0$ .

Since parity conservation in strong interactions requires that the  $\Lambda^0$  spin be normal to the  $\Lambda^0$  production plane, the angle  $\theta$  in Eq. (1) is identical to the angle  $\theta$  in our coordinate system. With use of this expression, the values for the  $\Lambda^0$  polarization were extracted from the data as follows. For each  $P_\perp$  bin, the binned data were fitted using  $\chi^2$  techniques to an angular distribution expressed as an expansion in spherical harmonics,  $A_{lm}Y_{lm}$ , weighted with the geometrical acceptance. The  $Y_{lm}$  are the normalized spherical harmonics and the  $A_{lm}$  are the coefficients. This fitting procedure was checked both by examination of Monte Carlo-generated samples with known polarization

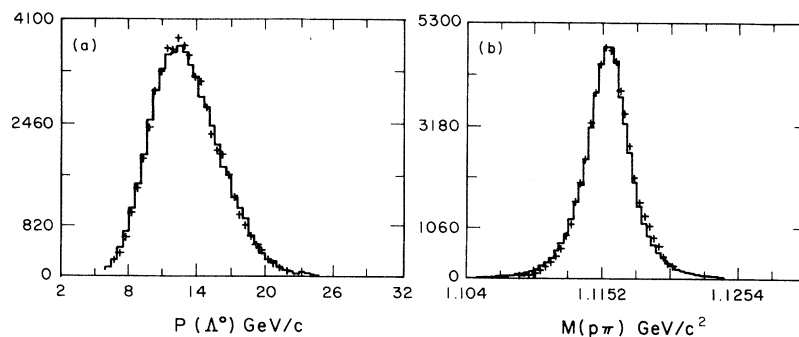


FIG. 2. (a) Momentum spectrum for the  $\Lambda^0$ 's. (b) Invariant  $p\pi^-$  mass spectrum for all events satisfying cuts. The data are indicated by the solid curve and the Monte Carlo-generated events are indicated by the plusses.

and by determination of the apparent polarization of the  $K_s^0 \rightarrow \pi^+\pi^-$  sample (found to be consistent with zero as expected.)<sup>9</sup> The fit to the data only required two terms,  $Y_{00}$  and  $Y_{10}$ , as expected from Eq. (1). The average  $\chi^2$  for these fits was 19.98 for eighteen degrees of freedom (confidence limit 0.4). The value of the polarization in each  $P_\perp$  bin is calculated as the ratio of the coefficients of the expansion

$$\mathcal{P} = A_{10}\sqrt{3}/A_{00}\alpha. \quad (2)$$

The  $\Lambda^0$  polarization as a function of  $P_\perp$  is shown in Fig. 3. The measured  $K \rightarrow \pi^+\pi^-$  contamination in the  $\Lambda^0$  sample was  $(0.4 \pm 0.1)\%$ . The values of the polarization presented in Fig. 3 have not been corrected for this negligible contamination.

The measured polarization did not change when the angular distribution was expanded to include terms out to  $Y_{22}$ . The polarization was also found to be independent of reasonable variations in all of the cuts applied to the data. In addition, the values were found to be insensitive to such possible systematic effects as slight mismeasurements of the track momenta or uncertainties in the location of the production target. No systematic effect was discovered which could change the result.<sup>10</sup> Our quoted errors represent equal contributions from the statistics of the data and Monte Carlo.

In Fig. 3 we also present other recent measurements of  $\Lambda^0$  polarization in inclusive production. For clarity, we plot only the high-statistics results at 400 GeV/c. We make the following ob-

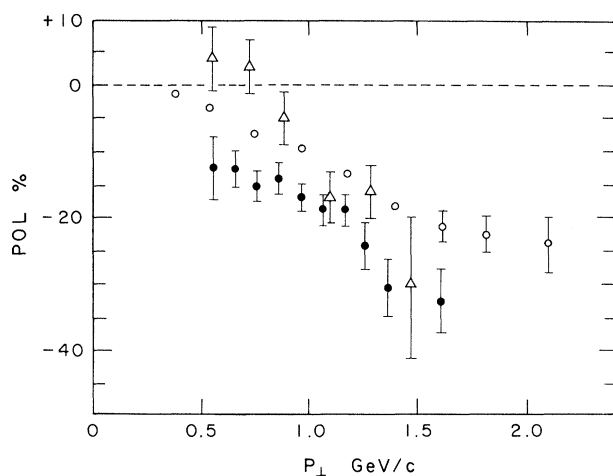


FIG. 3.  $\Lambda^0$  polarization vs transverse momentum (filled circles: this experiment, 28.5 GeV/c; inverted triangles: Ref. 2, 24 GeV/c; open circles: Ref. 3, 400 GeV/c).

servations. All of the experiments agree on the general features (including the sign) of the  $P_\perp$  dependence of the polarization. The polarization rises rapidly with  $P_\perp$  reaching a value of about  $-20\%$  at  $P_\perp = 1$  GeV/c. The polarization in the region  $0.55$  GeV/c  $< P_\perp < 1.6$  GeV/c is statistically consistent with a linear dependence on  $P_\perp$  although there appears to be a systematic curvature. When a detailed comparison is made between experiments, there are some significant differences. The polarization observed in this experiment (28.5-GeV/c protons on Ir) is significantly higher than the results at higher energy (300- or 400-GeV/c protons on Be).<sup>1,3</sup> This difference is most pronounced at low  $P_\perp$ . Specifically, the average polarization between 0.5 and 1.0 GeV/c from this experiment is  $(-14.9 \pm 0.9)\%$  compared with  $(-3.7 \pm 0.3)\%$  from the 400-GeV experiment. The difference at larger  $P_\perp$  is not as striking— $(-20.5 \pm 1.0)\%$  compared with  $(-17.1 \pm 0.7)\%$  although still significant. We also note that there are significant differences at small  $P_\perp$  with the measurement<sup>2</sup> at 24 GeV/c on platinum.

We note that a recent experiment<sup>11</sup> at the CERN intersecting storage rings observes  $\Lambda^0$  polarization in  $pp$  inclusive production which is larger than the results from the fixed-target experiment. It is important to note that all of the experiments on the hadronic inclusive production of  $\Lambda^0$ 's are unable to separate the contribution to the  $\Lambda^0$  polarization from  $\Sigma^0$  production.

We would like to thank F. Shoemaker of Princeton University for the loan of a large amount of equipment. Special thanks go to the Director and staff of Brookhaven National Laboratory without whose help this experiment could not have been done. We also thank the University of Massachusetts Computer Center for their assistance. This work was supported in part under Grants No. NSF PHY 76 84387 and No. NSF PHY 78 22997 from the National Science Foundation.

<sup>(a)</sup>Present address: Physics Department, Brandeis University, Waltham, Mass. 02154.

<sup>(b)</sup>Present address: 321 Conestoga Road, Wayne, Penn. 19087.

<sup>(c)</sup>Present address: Computerized Biomechanical Analysis, Inc., Amherst, Mass. 01002.

<sup>1</sup>G. Bunce *et al.*, Phys. Rev. Lett. **36**, 1113 (1976).

<sup>2</sup>K. Heller *et al.*, Phys. Lett. **68B**, 480 (1977).

<sup>3</sup>K. Heller *et al.*, Phys. Rev. Lett. **41**, 607 (1978).

<sup>4</sup>K. Heller, University of Michigan Report No. UM HE77-38, 1977 (to be published).

<sup>5</sup>B. Andersson *et al.*, Phys. Lett. **85B**, 417 (1979).

<sup>6</sup>G. Preparata, private communication.

<sup>7</sup>See for example, E. Commins, *Weak Interactions* (McGraw-Hill, New York, 1973).

<sup>8</sup>C. Bricman *et al.*, Phys. Lett. **75B**, i, 1 (1978).

<sup>9</sup>For a detailed discussion, see F. Lomanno, Ph.D. thesis, University of Massachusetts, Amherst, 1979

(unpublished).

<sup>10</sup>We note that possible  $\Lambda^\circ$  scattering in the Pb filter does not affect our result. Spin-flip scattering amplitudes must be zero at  $0^\circ$  and the pointback and geometrical cuts require that  $\Lambda^\circ$ 's in our sample pass through the filter essentially undeflected.

<sup>11</sup>S. Erhan *et al.*, Phys. Lett. **82B**, 301 (1979).

## Jets in Photon Collisions and Tests for a Pointlike Coupling of the Photon

A. Soni

Stanford Linear Accelerator Center, Stanford University, Stanford, California 94305, and  
Department of Physics, University of California, Irvine, Irvine, California 92717<sup>(a)</sup>

(Received 18 September 1979)

The pointlike coupling of the photon to the quark current yields simple predictions for the leading fast mesons in high- $p_t$   $\gamma N(LN)$ ,  $e^+e^-$ , and  $\gamma\gamma$  reactions, e.g., for  $\gamma p \rightarrow hX$  one gets  $K^+ : K^- : K^0 : \bar{K}^0 = 8:0:1:0$  and  $\pi^+ : \pi^- : \pi^0 = 8:1:\frac{1}{2}$ . It is noted that in  $\gamma N$  collisions the dominant jet cross section arises from the hard subprocess:  $\gamma + \text{gluon} \rightarrow q + \bar{q}$ . This may yield the gluon distribution via  $s \int s_0 (d\sigma/ds_0) K^{-1} = f_g(x)$  and lead to a sum rule:  $\int s_0^2 (d\sigma/ds_0) ds_0/sK = \int x f_g(x) dx$ , where  $K = 4\pi\alpha_s \ln(s/2p_{t\min}^2)$ .

In the context of the currently popular theory of strong interactions, i.e., quantum chromodynamics (QCD), the photon occupies a very special role<sup>1</sup> because it couples to quarks in a pointlike manner as dictated by quantum electrodynamics (QED). However, it is also an experimentally proven fact that for on-shell processes the photon possesses an important "hadronic" or vector-meson-dominated (VMD) component<sup>2</sup> which, e.g., can account for an overwhelming fraction of the total photon-nucleon cross section.<sup>3</sup> The VMD-model ideas are generally believed to be useful only for low-momentum-transfer reactions. The high-momentum-transfer phenomena are likely to be sensitive to the photon's pointlike coupling to the quark current.<sup>1,4</sup>

In this paper I suggest that an experimental study of photon-induced jets<sup>4</sup> and high- $p_t$  hadron production may be a valuable probe for detecting the presence of the pointlike component of the photon and for gaining a better understanding of the transition from the region of applicability of VMD to the pointlike coupling.<sup>5</sup> The interaction of the photon field with the quark current in proportion to their electric charge leads to simple predictions for ratios of mesons that are produced with a large  $p_t$  and carry a large fraction of the primary quark's energy. In addition, such reactions may elucidate the dynamics of the evolution of quark and gluon jets to hadrons and may yield quite directly the distribution function of the gluons in the nucleon.

Consider the photoproduction of hadrons at high transverse momentum. In lowest order of perturbative QCD these arise through two hard subprocesses: Photon-gluon fusion [Fig. 1(a)]

$$\gamma + g \rightarrow q + \bar{q} \tag{1}$$

and photon-induced Compton emission of gluons [Fig. 1(b)]

$$\gamma + q \rightarrow q + g. \tag{2}$$

With use of the quark-gluon coupling

$$\alpha_s(Q^2) = 12\pi/(33 - 2n_f) \ln Q^2/\Lambda^2, \tag{3}$$

one can compute the jet cross section for Eqs. (1) and (2). The results are shown in Fig. 2. I have taken  $\Lambda = 0.5$  GeV,  $m_{\text{quark}} = 0.3$  GeV, and set  $Q^2 = 4p_t^2$  ( $p_t$  is the transverse momentum of each jet with respect to the collision axis), and  $n_f = 3$ . In addition I have imposed  $p_t \geq p_{t\min} = 1.0$  GeV so as to confine the calculation to the region where both the pointlike coupling of the photon may domi-

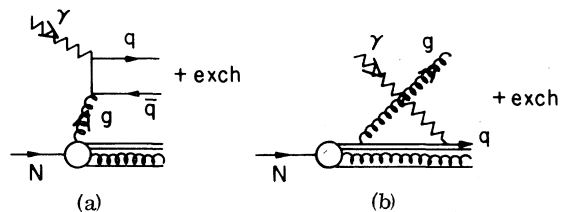


FIG. 1. Dominant hard subprocesses for photoproducing jets. (a) Pair-creation reaction (1)  $\gamma + g \rightarrow q + \bar{q}$ ; (b) Compton reaction (2)  $\gamma + q \rightarrow q + g$ .